

Aerosol lidar intercomparison in the framework of the EARLINET project. 1. Instruments

Volker Matthias, Volker Freudenthaler, Aldo Amodeo, Ioan Balin, Dimitris Balis, Jens Bösenberg, Anatoly Chaikovskiy, Georgios Chourdakis, Adolfo Comeron, Arnaud Delaval, Ferdinando De Tomasi, Ronald Eixmann, Arne Hågård, Leonce Komguem, Stephan Kreipl, Renaud Matthey, Vincenzo Rizi, José António Rodrigues, Ulla Wandinger, and Xuan Wang

In the framework of the European Aerosol Research Lidar Network to Establish an Aerosol Climatology (EARLINET), 19 aerosol lidar systems from 11 European countries were compared. Aerosol extinction or backscatter coefficient profiles were measured by at least two systems for each comparison. Aerosol extinction coefficients were derived from Raman lidar measurements in the UV (351 or 355 nm), and aerosol backscatter profiles were calculated from pure elastic backscatter measurements at 351 or 355, 532, or 1064 nm. The results were compared for height ranges with high and low aerosol content. Some systems were additionally compared with sunphotometers and starphotometers. Predefined maximum deviations were used for quality control of the results. Lidar systems with results outside those limits could not meet the quality assurance criterion. The algorithms for deriving aerosol backscatter profiles from elastic lidar measurements were tested separately, and the results are described in Part 2 of this series of papers [Appl. Opt. **43**, 977–989 (2004)]. In the end, all systems were quality assured, although some had to be modified to improve their performance. Typical deviations between aerosol backscatter profiles were 10% in the planetary boundary layer and $0.1 \times 10^{-6} \text{ m}^{-1} \text{ sr}^{-1}$ in the free troposphere. © 2004 Optical Society of America

OCIS codes: 280.1100, 280.3640, 290.1350, 290.2200, 290.5860.

When the research was conducted, V. Matthias was with the Max-Planck-Institut für Meteorologie, Bundesstrasse 55, 20146 Hamburg, Germany; V. Freudenthaler was with the Meteorologisches Institut, Ludwig-Maximilians—Universität München, Theresienstrasse 37, 80333 Munich, Germany; A. Amodeo was with the Istituto di Metodologie per l'Analisi Ambientale, Consiglio Nazionale delle Ricerche, Contrada S. Loja, 85050 Tito Scalo (Potenza), Italy; I. Balin was with the Laboratoire de Pollution de l'Air et du Sol, École Polytechnique Fédérale de Lausanne, 1015 Lausanne, Switzerland; D. Balis was with the Laboratory of Atmospheric Physics, Aristotle University of Thessaloniki, Box 149, 54124 Thessaloniki, Greece; J. Bösenberg was with the Max-Planck-Institut für Meteorologie, Bundesstrasse 55, 20146 Hamburg, Germany; A. Chaikovskiy was with the Institute of Physics National Academy of Sciences of Belarus, 68 F. Scarina Avenue, 220072 Minsk, Belarus; G. Chourdakis was with the Department of Physics, National Technical University of Athens, Heroon Polytechniou 9, 15780 Zografou, Greece; A. Comeron was with the Universitat Politècnica de Catalunya, Jordi Girona 1 y 3. Edif. D3-202, 08034 Barcelona, Spain; A. Delaval was with the Institute Pierre Simone Laplace, Laboratoire de la Météorologie Dynamique, 91128 Pal-

Received 19 March 2003; revised manuscript received 1 October 2003; accepted 10 November 2003.

0003-6935/04/040961-16\$15.00/0

© 2004 Optical Society of America

aiseau Cedex, France; F. De Tomasi was with the Istituto Nazionale per la Fisica della Materia, Dipartimento di Fisica, Università di Lecce, via Arnesano, 73100 Lecce, Italy; R. Eixmann was with the Leibniz-Institut für Atmosphärenphysik, Schloßstrasse 6, 18225 Kühlungsborn, Germany; A. Hågård was with the Division of Sensor Technology, Swedish Defence Research Agency, P.O. Box 1165, 58111 Linköping, Sweden; L. Komguem was with the Department of Physics, University of Wales, Aberystwyth Ceredigion SY23 3BZ, UK; S. Kreipl was with the Institut für Meteorologie und Klimaforschung, Forschungszentrum Karlsruhe, Kreuzackbahnstrasse 19, 82467 Garmisch-Partenkirchen, Germany; R. Matthey was with the Observatoire de Neuchâtel, Rue de l'Observatoire 58, 2000 Neuchâtel, Switzerland; V. Rizi was with the Dipartimento di Fisica, Università degli Studi—L'Aquila, Via Vetoio Località Coppito, 67010 L'Aquila, Italy; J. A. Rodrigues was with the Centro de Física de Plasmas, Instituto Superior Técnico, Avenida Rovisco Pais, 1049-001 Lisboa, Portugal; U. Wandinger was with the Institute for Tropospheric Research, Permoserstrasse 15, 04303 Leipzig, Germany; and X. Wang was with the Istituto Nazionale per la Fisica della Materia, Complesso Universitario di Monte S. Angelo, via Cintia, 80126 Naples, Italy. V. Matthias (matthias@gkss.de) is now with the Institute for Coastal Research, GKSS Research Center, Max-Planck-Strass 1, 21502 Geesthacht, Germany.

1. Introduction

The European Aerosol Research Lidar Network to Establish an Aerosol Climatology (EARLINET) is a joint project that comprises 19 European lidar systems from 11 countries.¹ The main goal of the project is to provide a quantitative, statistically relevant data set of the vertical aerosol distribution over Europe. For this purpose regular measurements were taken on preselected days of the week, regardless of weather conditions. Generally, only rain and very low clouds (cloud base below ~800 m) prevented our taking lidar measurements.

Additional measurements with which to investigate special aerosol events such as Saharan dust outbreaks, forest fires, and photochemical smog episodes are being performed. Long-range transport of aerosols from, e.g., North America to Europe and the lifting of aerosol particles in the Alpine region are other special tasks of the project. Aerosol source regions and the modification of aerosol as it traverses Europe are studied by use of the lidar profiles together with backtrajectories provided by the German Weather Service.

The groups of scientists who are participating in this study (with the abbreviations for the names of those groups in parentheses) are the following:

- Department of Physics of the University of Wales, Aberystwyth, UK (ab),
- National Technical University of Athens, Athens, Greece (at),
- Universitat Politècnica de Catalunya, Barcelona, Spain (ba),
- Institut für Meteorologie und Klimaforschung, Garmisch-Partenkirchen, Germany (gp),
- Max-Planck-Institut für Meteorologie, Hamburg, Germany (hh),
- Ecole Polytechnique Fédérale de Lausanne, Lausanne, Switzerland (ju),
- Institut für Atmosphärenphysik, Kühlungsborn, Germany (kb),
- Dipartimento di Fisica, Università Degli Studi, L'Aquila, Italy (la),
- Istituto Nazionale per la Fisica della Materia, Lecce, Italy (lc),
- Institut für Troposphärenforschung, Leipzig, Germany (le),
- Instituto Superior Técnico, Lisbon, Portugal (li),
- Försvarets Forsknings Institut Linköping, Sweden (lk),
- Institute of Physics, Academy of Sciences of Belarus, Minsk, Belarus (mi),
- Meteorologisches Institut der Ludwig-Maximilians-Universität München, Munich, Germany (mu),
- Istituto Nazionale per la Fisica della Materia, Naples, Italy (na),
- Observatoire Cantonal Neuchâtel, Neuchâtel, Switzerland (ne),
- Laboratoire de la Météorologie Dynamique, Institute Pierre Simon Laplace, Palaiseau, France (pl),

- Istituto di Metodologie per l'Analisi Ambientale, Potenza, Italy (po),
- Aristotle University of Thessaloniki, Thessaloniki, Greece (th),
- Institut für Mathematik der Universität Potsdam, Potsdam Germany.

All groups whose abbreviations appear in parentheses operate aerosol lidar systems on a routine basis. The University of Potsdam is involved in the algorithm intercomparison and in the development of new retrieval algorithms to get microphysical aerosol information from multiwavelength lidar measurements.

The statistical evaluation of aerosol profiles from 19 sites taken over almost 3 years requires a high standard for the measuring instruments. To check the performance and reliability of the individual lidar systems, intercomparison measurements were made. Comparing the results of two lidar systems located close together and therefore probing nearly the same volume of air is regarded as the best way to determine the precision of an aerosol lidar. In the past, lidar intercomparisons had been performed mainly by trace gas measurement in the field. Ozone differential absorption lidar systems were compared to electrochemical balloonsondes in the troposphere,² either free-flying or tethered sondes, and to helicopter-based *in situ* ozone monitors.^{3,4} In the stratosphere, balloonsondes, rocket sondes, and satellite measurements were used for intercomparisons.^{5,6} Water-vapor lidars, especially true Raman lidars, had frequently been compared to free-flying radiosondes, because the necessary calibration of the systems is similar.^{7,8} Water-vapor DIAL systems had also been compared to tethered balloonsondes and other passive remote sensors, with good results.⁹ In a few cases intercomparisons of lidar systems, either ozone or water-vapor lidars, were made.^{10,11}

Trace gases such as ozone and water vapor can be measured with balloonborne sondes. Therefore independent measurements are available to test the quality of the lidar measurements. For aerosol lidars the situation is much more complex. Intercomparisons made by different instruments measuring vertically resolved aerosol backscatter or extinction are difficult, to reconcile. Making airborne measurements at 19 different lidar sites over Europe is an expensive and difficult undertaking. Additionally, comparison with *in situ* instruments such as nephelometers suffer from numerous difficulties, including differences in wavelengths, in probed air volumes, in humidity of the probed aerosols, and in observed size distributions among the various instruments. Therefore the intercomparisons generally remain qualitative^{12,13} or depend on correct assumptions about the single-scattering albedo or the aerosol's refractive index.¹⁴ Comparisons of optical depth can be made with passive instruments such as photometers¹⁵⁻¹⁷ in this case, however, horizontal homogeneity of the aerosol distribution and an absence of clouds are required. Additionally, vertical distributions of aerosols cannot be measured with these

Table 1. Properties of EARLINET Lidar Systems

Abbreviation for Lidar Group	Elastic Channel (nm)			Raman Channel		Transportation System
	355	532	1064	387	607	
ab	Yes			Yes		
at	Yes	Yes		Yes		
ba		^a	Yes			Yes
hh ^b	Yes	Yes	Yes	Yes		Yes
gp	Yes	Yes	Yes			Yes
ju	Yes	Yes	Yes	Yes		
kb	Yes	Yes	Yes	Yes	Yes	
la	Yes ^c			Yes ^d		
lc	Yes ^c			Yes ^d		
le	Yes	Yes	Yes	Yes	Yes	Yes ^e
li		^a	Yes			Yes
lk	Yes					Yes
mi	Yes ^f	Yes	Yes			
mu	Yes	Yes	Yes			Yes
na	Yes ^c			Yes ^d		
ne	Yes	Yes	Yes			Yes ^g
pl		Yes	Yes			
po	Yes	Yes		Yes		
th	Yes	Yes		Yes		

^aUpgrade of this channel was completed during the EARLINET.

^bUntil September 2000 the system was emitting only at 351 nm.

^cEmitted wavelength, 351 nm.

^dDetected wavelength, 382 nm.

^eRoutine measurements are performed with a stationary system.

^fEmitted wavelength, 353 nm.

^gThe transportable system emits only 532 nm.

instruments. Because of these difficulties, significant intercomparisons of aerosol lidars had not been made previously. For the EARLINET, direct intercomparisons of a tested lidar system with a second system were regarded as the best way to ensure the quality of the aerosol lidar profiles. This conclusion led to the largest lidar intercomparison campaign so far, including 19 different aerosol lidar systems, as we report here.

We separately tested the algorithms used by the various groups of lidar systems to distinguish between errors based on technical problems of the systems and those based on the algorithms. The results of the aerosol backscatter algorithm intercomparison are presented in Part 2 of this series of papers.¹⁸ Algorithms with which to derive aerosol extinction, backscatter, and lidar ratio from Raman lidar measurements also were tested. These results will be published as Part 3 of the aerosol lidar intercomparisons in the framework of the EARLINET.¹⁹

2. Lidar Systems

EARLINET aerosol lidar measurements are usually performed at three standard wavelengths: one in the UV (at either 355 or 351 nm), one in the green (532 nm), and one in the IR (1064 nm) spectral region. Those wavelengths are common in systems that are based on the widely used flash-lamp-pumped pulsed Nd:YAG lasers. The second UV wavelength, at 351 nm, is emitted by the also widely used XeF excimer laser. However, not all systems are operated at

three wavelengths: Some use only 532 and 1064 nm; others use 355 and 532 nm. The excimer-based systems are single-wavelength systems.

Most of the lidar groups installed additional Raman channels in the UV to detect nitrogen Raman backscatter at either 382 nm (excimer laser) or 387 nm (Nd:YAG laser). UV wavelengths were preferably chosen as Raman channels because the Raman backscattering cross section is higher than in the visible, and detectors with high sensitivity and low dark current can be found in that wavelength region. Few systems have a second Raman channel in the green to detect also nitrogen Raman backscatter from 532 nm at 607 nm. Table 1 gives a brief overview of the various systems.

Only some of the systems are transportable. This is an important restriction for intercomparison experiments. Additionally, only two of the transportable systems are equipped with Raman channels, because detection of Raman backscatter usually requires high-power lasers, which are much larger and consume more power than those used for pure backscatter measurements. These Raman lidar systems are installed in 20-ft (~608-m) containers; the other transportable systems have much smaller sizes.

All systems had already existed before the start of the EARLINET in 2000. Therefore the network comprises a large variety of lidar systems, which were all constructed by the respective operating institutions. Some of these systems (e.g., those at the

Ecole Polytechnique Fédérale de Lausanne, located at Jungfraujoch at 3580 m above sea level (asl), from the Institut für Atmosphärenphysik, Kühlungsborn, and from Dipartimento di Fisica, Università Degli Studi, L'Aquila) were originally constructed to probe the upper troposphere and the lower stratosphere. For this reason some systems do not always cover the planetary boundary layer where most of the aerosol can be found.

3. Data Analysis

A. Aerosol Backscatter

Aerosol backscatter measurements are based on the detection of pure elastic backscatter from emitted laser light. The algorithms used for the retrieval of aerosol backscatter profiles follow the publications of Klett,^{20,21} Fernald *et al.*,²² and Fernald.²³ To solve the lidar equation in the simplest case of no

or an atmospheric density profile from nearby launched radiosondes, $\alpha_{aer}(\lambda, z)$ and $\beta_{aer}(\lambda, z)$ remain as two height-dependent unknowns while one signal is measured. One usually solves this problem by assuming an (*a priori* unknown) relationship between aerosol backscatter and extinction. $S_{aer}(\lambda, z) = \alpha_{aer}(\lambda, z)/\beta_{aer}(\lambda, z)$ is usually called the lidar ratio; it depends on wavelength and height. The determination of $\beta_{aer}(z)$ from Eq. (1) for one wavelength requires the additional assumption of an unknown constant that represents the height-independent system parameters. To determine this constant and solve Eq. (1) for $\beta_{aer}(z)$, usually a so-called calibration or reference value $\beta_{aer}(\lambda, z_0)$ is chosen that prescribes the aerosol backscatter at a specific height z_0 .

From these assumptions the equation for $\beta_{aer}(z)$ can be solved. Following Fernald *et al.*²² and Fernald,²³ one gets for all heights where $z_0 > z$ (calibration in the far range)

$$\beta_{aer}(z) = -\beta_{mol}(z) + \frac{P(z)z^2 \exp\left[-2(S_{aer} - S_{mol}) \int_0^z \beta_{mol}(\zeta) d\zeta\right]}{P_0 C - 2S_{aer} \int_0^z P(\zeta)\zeta^2 \exp\left[-2(S_{aer} - S_{mol}) \int_0^\zeta \beta_{mol}(z') dz'\right] d\zeta}, \quad (2)$$

gaseous absorption it is useful to split backscatter and extinction into their molecular and aerosol parts and to use only that part of the profile where

where $S_{mol} = \alpha_{mol}(\lambda, z)/\beta_{mol}(\lambda, z) = 8\pi/3$. Calibration at height z_0 gives the system constants $P_0(\lambda)C$. Writing $X(z) = P(z)z^2$ gives

$$\beta_{aer}(z) = -\beta_{mol}(z) + \frac{X(z) \exp\left[-2(S_{aer} - S_{mol}) \int_0^z \beta_{mol}(\zeta) d\zeta\right]}{[X(z_0)/\beta_{aer}(z_0) + \beta_{mol}(z_0)] - 2S_{aer} \int_0^\zeta X(\zeta) \exp\left[-2(S_{aer} - S_{mol}) \int_{z_0}^\zeta \beta_{mol}(z') dz'\right] d\zeta}. \quad (3)$$

the laser beam fully overlaps the field of view of the receiving telescope:

$$P(\lambda, z) = P_0(\lambda)C \frac{\beta_{aer}(\lambda, z) + \beta_{mol}(\lambda, z)}{z^2} \times \exp\left\{-2 \int_0^z [\alpha_{aer}(\lambda, \zeta) + \alpha_{mol}(\lambda, \zeta)] d\zeta\right\}; \quad (1)$$

where $P_0(\lambda)$ and $P(\lambda, z)$ are the emitted and received powers, respectively, C combines the system constants, $\beta(\lambda, \zeta)$ denotes the backscatter coefficient, and $\alpha(\lambda, \zeta)$ is the extinction coefficient at wavelength λ and range z . ζ is used here as the integration variable over height.

Assuming that the molecular part of Eq. (1) can be calculated by use of standard atmosphere conditions

Then Eq. (3) can be solved iteratively downward or upward from z_0 . Molecular absorption is neglected here. Molecular scattering can be calculated with sufficient accuracy by use of actual radiosonde measurements or ground values of temperature and pressure and standard atmosphere conditions.^{24–26} The particle lidar ratio and the particle backscatter coefficient $\beta_{aer}(z_0)$ at a suitable reference height z_0 have to be estimated in the determination of the particle backscatter coefficient profile after Eq. (3). The numerical application of Eq. (3) has been discussed in the literature for more than 20 years. Contributions to the solution of the problem have also been made by Sasano *et al.*,²⁷ Kovalev and Moosmüller,²⁸ Matsumoto and Takeuchi,²⁹ and Bösenberg *et al.*³⁰

B. Aerosol Extinction

To overcome the problem of aerosol profiles that are based on the assumption of an *a priori* unknown lidar

ratio, one measures aerosol extinction by detecting the inelastic Raman backscatter from atmospheric nitrogen at λ_R , if λ_0 is the emitted wavelength. Solving a Raman lidar equation for the aerosol extinction term leads to³¹

$$\alpha_{aer,z}(\lambda_0) = \frac{1}{1 + (\lambda_0/\lambda_R)^k} \times \frac{d}{dz} \ln \left[\frac{N(z)}{P_R(z)z^2} \right] - \alpha_{mol}(\lambda_0, z) - \alpha_{mol}(\lambda_R, z), \quad (4)$$

where $N(z)$ is the atmospheric density of the Raman scatterer and k is the Ångström exponent that describes the wavelength dependence of aerosol extinction by $\alpha_{aer} \propto \lambda^{-k}$.

One can also use the information about the aerosol extinction to derive the aerosol backscatter without assuming a lidar ratio. One usually calculates the backscatter profile by forming the ratio of the elastic and the Raman backscattered signals in height z and calibration height z_0 . As for the pure elastic backscatter, one eliminates the system constants by choosing a calibration value $\beta_{aer}(z_0)$ for the aerosol backscatter in height z_0 . When accurate calibration of the backscatter profile at a height with negligible aerosol backscatter is possible, the lidar ratio can also be calculated.

4. Methods of Quality Assurance

A. Organization

As early as in 1998, intercomparisons on an instrument level were performed with four of the German lidars in the framework of the German Aerosol Lidar Network.³² These lidars were regarded as quality assured from the beginning of the EARLINET. Two of these lidars performed most of the intercomparison experiments by travelling to different sites in Europe; these were the systems from the Max Planck Institute for Meteorology in Hamburg (MPI) and from the Meteorological Institute of the Ludwig Maximilians University of Munich (MIM). Both systems emit three laser wavelengths, in the UV (355 nm), the green (532 nm), and the IR (1064 nm). The MPI system is additionally equipped with a Raman channel at 387 nm. Many of the systems within the EARLINET project are not transportable; therefore it was not possible to perform one big intercomparison experiment with all systems at one site. The largest experiment, with five systems performed in September 2000 in Palaiseau, France, was the starting point for several pairwise intercomparisons at different sites. Most of the experiments were done in September and October 2000 with the Munich system traveling to Italy and Greece. Other experiments followed in the spring and summer of 2001.

Each system that was successfully compared with a quality-controlled system was regarded as quality controlled itself and could therefore be compared with another system. This kind of quality control was

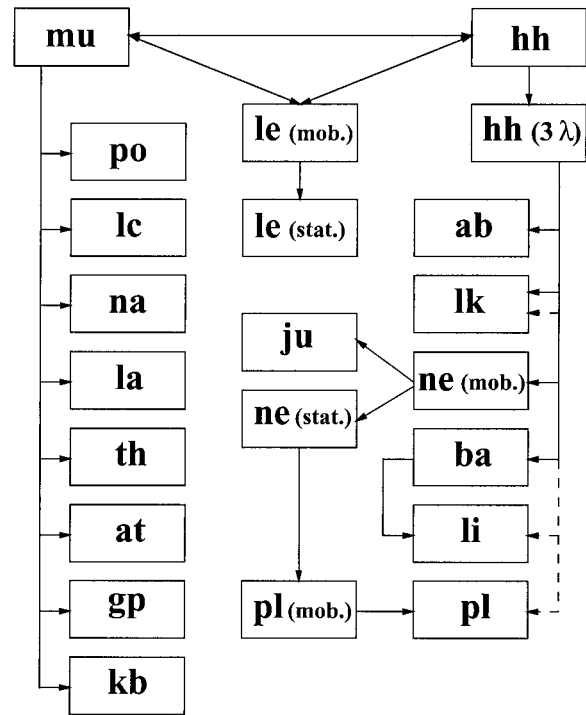


Fig. 1. Diagram of intercomparison experiments performed for EARLINET quality assurance. The systems from Linköping (lk), Lisbon (li), and Palaiseau (pl) had to repeat the intercomparisons: (mob.), mobile microlidar; (stat.), stationary system.

used for the intercomparisons in Barcelona, Neuchâtel, and on the Jungfraujoch. An exception to this rule was allowed for the group in Minsk (Belarus). Traveling with a lidar system to that site was regarded as impossible. Therefore internal intercomparisons with two of their systems at 532 nm were made in Minsk.

Three systems had to repeat the intercomparison experiment because the first measurements were not usable for technical reasons and the problems could not be solved within a few days during the measurement campaign. The new measurements were performed in the summer of 2001 and in the summer and fall of 2002. Figure 1 illustrates the intercomparison procedure and shows which systems were measured simultaneously. The group from Palaiseau used a mobile microlidar to perform its new intercomparisons. First its system was compared with the stationary system in Neuchâtel before it was used for the intercomparisons with the stationary system in Palaiseau. The dates of the individual experiments are displayed in Table 2.

B. Quality Criteria

The quality criteria were fixed in advance. Experimentally derived deviations among the lidar systems from Hamburg, Munich, and Leipzig during the intercomparison in 1998³² were taken together with results from a separately performed algorithm intercomparison¹⁸ to define upper limits for mean and standard deviations at several wavelengths. All

Table 2. Dates and Places of the EARLINET Intercomparison Experiments

Lidar Group	Compared with	Date	Place	Comment
ab	hh	5/2001	Aberystwyth	Includes extinction
at	mu	9/2000	Athens	
ba	hh	9/2000	Palaiseau	
gp	mu	7/2001	Munich	
ju	ne	5/2001	Jungfrauoch	With Neuchâtel microlidar
kb	mu	8/1998	Kühlungsborn	Within the German Lidar Network
la	mu	10/2000	L'Aquila	
lc	mu	10/2000	Lecce	
le	mu, hh	8/1998	Lindenberg	Within the German Lidar Network
li	hh	9/2000	Palaiseau	New intercomparisons in Barcelona in 6/2002
lk	hh	10/2000	Hamburg	New intercomparisons in Hamburg in 8/2001
mi	internal	4-6/2000	Minsk	Using two systems from Minsk
na	mu	10/2000	Naples	
ne	hh	9/2000	Palaiseau	With Neuchâtel microlidar
ne	ne	4-5/2001	Neuchâtel	Neuchâtel stationary with microlidar
pl	hh	9/2000	Palaiseau	New intercomparisons in Neuchâtel in 6/2002
po	mu	10/2000	Potenza	
th	mu	9/2000	Thessaloniki	

groups agreed on reaching these values during the intercomparisons.

The mean value \bar{m} of an observed quantity m is defined as

$$\bar{m} = \frac{\sum_{i=1}^n m}{n} \quad (5)$$

if n values are given in a certain height range. If the difference between two profiles at a given height is $\Delta m = m_1 - m_2$, the mean deviation between the profiles is

$$\overline{\Delta m} = \frac{\sum_{i=1}^n \Delta m}{n} \quad (6)$$

if, again, n values are compared. Then the relative mean deviation (in percent) is

$$\overline{\Delta m}_{rel} = 100 \times \frac{\overline{\Delta m}}{\bar{m}}. \quad (7)$$

Finally, the standard deviation is calculated as

$$\delta m = \left[\frac{\sum_{i=1}^n (\Delta m)^2}{n - 1} \right]^{1/2} \quad (8)$$

and the corresponding relative value (in percent) is

$$\delta m_{rel} = 100 \times \frac{\delta m}{\bar{m}}. \quad (9)$$

The aim of each intercomparison experiment was to derive several aerosol extinction and backscatter profiles from all participating lidar systems under different atmospheric conditions with different aerosol loads. The lidar systems were located very close together, with a horizontal distance of less than 500 m. Each compared profile was typically averaged over

15–30 min in time and 50–300 m in space. The amount of aerosol in the atmosphere for at least two measurements had to be moderate or high, which meant using the following values: $\beta_{max} > 3 \times 10^{-6} \text{ m}^{-1} \text{ sr}^{-1}$ at 355 nm and $\alpha_{max} > 2 \times 10^{-4} \text{ m}^{-1}$ at 355 nm, to ensure values well above the detection limit. We scaled these values down to longer wavelengths, assuming an $\alpha, \beta \propto \lambda^{-1}$ dependence. The requirements on α_{max} and β_{max} included that all systems were able to perform measurements within the planetary boundary layer where the highest aerosol load can be found. Both nighttime and daytime measurements were compared, especially when significant differences in daytime and nighttime operation could be expected.

C. Compared Quantities

Compared quantities were (if measured)

- Aerosol backscatter at 355, 532, and 1064 nm,
- Aerosol extinction at 355 nm, and
- Aerosol optical depth (comparison with aerosol optical depth from sunphotometer or starphotometer).

To compare aerosol backscatter profiles calculated with an inversion algorithm (Section 3) we used equal lidar ratio profiles $S_{aer}(z)$ and aerosol backscatter calibration values $\beta_{aer}(z_0)$. For extinction profiles derived from the Raman method, equal Ångström coefficients k were taken and all corrections to the measured signals (e.g., dead-time correction, overlap correction) were applied by the individual lidar systems before the intercomparison. For the determination of optical depth from aerosol extinction profiles, well-mixed conditions with constant aerosol extinction in the layer between ground and the lower end of the profile were assumed. Then the profile was integrated over the whole height range. To

Table 3. Maximum Allowed Relative and Absolute Deviations for the Compared Quantities

Quantity	Mean Deviation	Standard Deviation	Minimum Height Interval (m)
Aerosol Extinction (355 nm)	<20%/0.5 × 10 ⁻⁴ m ⁻¹	<25%/1.0 × 10 ⁻⁴ m ⁻¹	1000
Aerosol backscatter			
355 nm	<20%/0.5 × 10 ⁻⁶ m ⁻¹ sr ⁻¹	<25%/0.5 × 10 ⁻⁶ m ⁻¹ sr ⁻¹	2000
532 nm	<20%/0.5 × 10 ⁻⁶ m ⁻¹ sr ⁻¹	<25%/0.5 × 10 ⁻⁶ m ⁻¹ sr ⁻¹	2000
1064 nm	<30%/0.5 × 10 ⁻⁶ m ⁻¹ sr ⁻¹	<30%/0.5 × 10 ⁻⁶ m ⁻¹ sr ⁻¹	2000
Aerosol optical depth (355 nm)	<30%/0.1	<30%/0.1	2000

compare nighttime measured Raman extinction profiles with daytime sunphotometer measurements we allowed time differences of as much as 3 h, assuming a stable meteorological situation with no horizontal advection of a different air mass during this time. We could verify this stability by looking at the temporal development of the lidar signals.

D. Maximum Deviations

An intercomparison was regarded as successful if the deviation between the system and the quality controlled system was in a given interval below one of the values given in Table 3. Profiles were split into regions with high aerosol load and low aerosol load to permit the requirements for each interval to be fitted separately. The region with the high aerosol load will usually be the planetary boundary layer (PBL), and we shall use this name here without further distinction between, e.g., the mixing layer and the residual layer. The region above the PBL, with the low aerosol load, is called the free troposphere. In the PBL it is useful to give relative mean deviations and standard deviations according to Eq. (7) and (9). To pass the quality-assurance criterion in the PBL the calculated deviations had to stay below one of the given limits, either the relative or the absolute deviation. In regions such as the free troposphere with low aerosol content, mean and standard deviations are given in absolute numbers only. For low aerosol backscatter, relative numbers can easily reach a few hundred percent, although the absolute deviations will remain small and therefore are not used here.

5. Experiments and Results

Although each intercomparison experiment was scheduled for 3–5 days, measurements under different meteorological conditions could not be taken in every case. Sometimes also the minimum aerosol backscatter and extinction values could not be reached because of the advection of clean air over several days or special conditions at mountain sites such as the Jungfrauoch, which is 3580 m asl. In three cases, technical problems had to be solved also before further measurements could be taken. Therefore the intercomparisons in 15 of 19 cases were restricted to three episodes, at least one of which has a high aerosol load.

A. Intercomparison of Lidar Systems

In total, 146 aerosol backscatter profiles were compared. Mean and standard deviations were calculated and tested with respect to the quality criteria. Not all profiles are displayed here, but some typical results are discussed in detail. They show the good performance of most of the systems; but problems and limitations are also discussed.

All profiles were calculated only in a height region where full overlap between the emitted laser beam and the receiving telescope’s field of view was expected. An overlap function to correct the aerosol backscatter values in the region of incomplete overlap was not applied in any of the cases. Nevertheless, some minor near-range deviations between the compared profiles could still be due to incomplete overlap. The compared profiles were taken within exactly the same time window. Appropriate vertical averaging was chosen by each lidar system individually. The signal statistics can be quite different among the systems, depending on laser power, detector efficiency, and optical arrangement. So, whenever possible, sufficient temporal averaging was applied to prevent large deviations owing to statistical signal errors.

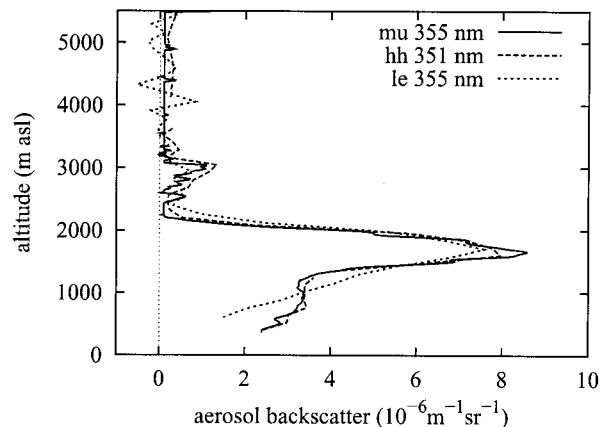


Fig. 2. Intercomparison of aerosol backscatter profiles at 351 and 355 nm of the lidar systems from Leipzig (le), Munich (mu), and Hamburg (hh). Measurements were taken on 11 August 1998 at 21:15–21:45 UT during the LACE 98 experiment.

Table 4. Leipzig and Munich Backscatter Intercomparisons^a

Date (UT)	Wavelength (nm)		Height Range (m)	Mean Deviation ($\times 10^{-6} \text{ m}^{-1} \text{ sr}^{-1}$)	Standard Deviation ($\times 10^{-6} \text{ m}^{-1} \text{ sr}^{-1}$)
09/08/1998 (22:30–23:00)	532		600–1300	0.04/7.7%	0.30/27.1%
			1500–3000	–0.03	0.09
11/08/1998 (12:07–12:12)	532		500–3200	0.07/8.6%	0.16/12.6%
11/08/1998 (21:15–21:45)	355		600–2000	0.38/11.3%	0.70/18.5%
			2400–3800	–0.06	0.22
11/08/1998 (21:15–21:45)	532		600–2000	0.23/2.9%	0.56/17.2%
			2400–3800	0.15	0.32
11/08/1998 (21:15–21:45)	1064		600–2000	0.07/5.6%	0.10/9.3%
			2400–4300	–0.09	0.10

^aAllowed absolute mean deviations and standard deviations are $0.5 \times 10^{-6} \text{ m}^{-1} \text{ sr}^{-1}$ at all wavelengths. Allowed relative mean (and standard) deviations in the PBL are 20% (25%) at 355 and 532 nm and 30% (30%) at 1064 nm.

1. Aerosol Backscatter

Most of the compared profiles were aerosol backscatter profiles in the UV (351 or 355 nm) and the green (532 nm). Two MPI systems were part of the intercomparison experiments shown here. In 1998 the MPI system was excimer based, emitting at 351 nm, because in the year 2000 the MPI also operated a three-wavelength Nd:YAG-based system that performed the intercomparisons in 2000 and 2001. It was compared with the excimer system during separate measurements in Hamburg. The MIM system remained unchanged in its optical design from 1998 to 2001. The dynamic range of the system could be extended by use of a new data acquisition system.

a. Leipzig–Munich–Hamburg Data

The measurements by the three German lidar groups from Leipzig, Munich, and Hamburg were performed in August 1998 during the Lindenberg Aerosol Characterization Experiment (LACE 98).¹⁷

The results of measurements from 11 August 1998 at 21:15–21:45 UT can be seen in Fig. 2. Two height ranges, 600–2000 m with a high aerosol load and 2400–3800 m with a low aerosol load, were distinguished for calculation of the mean differences and their standard deviations. In both height ranges the agreement was good and the deviations stayed well below the allowed values (see Tables 4–6). The backscatter profile from the Institute for Tropospheric Research (IFT), Leipzig, shows some small deviations in the lowest altitudes, which are probably due to incomplete overlap between the laser beam and the telescope’s field of view. This is the typical near-range effect of systems that are equipped with large receiving mirrors. The IFT system covers the lowest range by tilting the laser beam and the telescope to lower elevation angles.³³ This measurement was made for an elevation angle of 50°; the MPI and the MIM systems were vertically pointing. The MPI system was excimer-laser based, emitting laser light at 351

Table 5. Munich and Hamburg Backscatter Intercomparisons^a

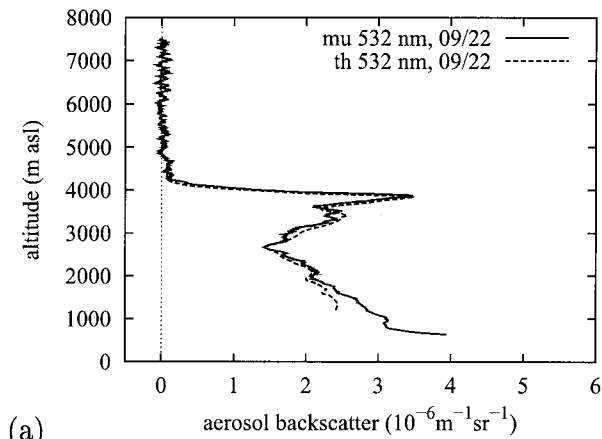
UT on 11/08/1998	Wavelength (nm)		Height Range (m)	Mean Deviation ($\times 10^{-6} \text{ m}^{-1} \text{ sr}^{-1}$)	Standard Deviation ($\times 10^{-6} \text{ m}^{-1} \text{ sr}^{-1}$)
	Munich	Hamburg			
12:07–12:12	355	351	500–3200	0.43/16.1%	0.59/19.7%
21:15–21:45	355	351	600–2000	0.01/1.5%	0.26/7.5%
			2400–3800	–0.04	0.2

^aAllowed absolute mean deviations and standard deviations are $0.5 \times 10^{-6} \text{ m}^{-1} \text{ sr}^{-1}$. Allowed relative mean (and standard) deviations in the PBL are 20% (25%).

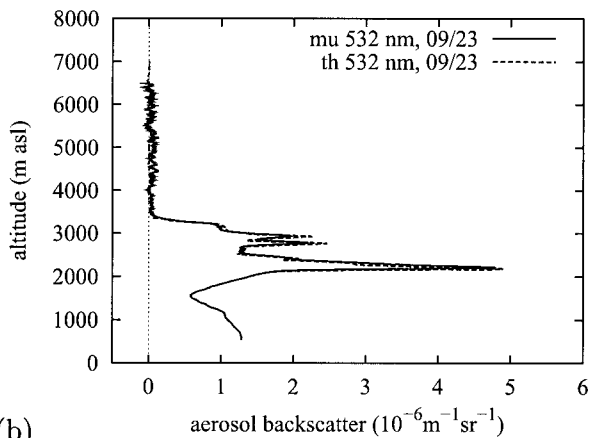
Table 6. Leipzig and Hamburg Backscatter Intercomparisons^a

Date (UT)	Wavelength (nm)		Height Range (m)	Mean Deviation ($\times 10^{-6} \text{ m}^{-1} \text{ sr}^{-1}$)	Standard Deviation ($\times 10^{-6} \text{ m}^{-1} \text{ sr}^{-1}$)
	Leipzig	Hamburg			
09/08/1998 (22:30–23:00)	355	320	600–1300	0.38/39.0%	0.48/53.0%
			1600–3000	0.13	0.14
11/08/1998 (21:15–21:45)	355	351	600–2000	0.38/12.9%	0.62/16.2%
			2400–3800	0.15	0.32

^aAllowed absolute mean deviations and standard deviations are $0.5 \times 10^{-6} \text{ m}^{-1} \text{ sr}^{-1}$. Allowed relative mean (and standard) deviations in the PBL are 20% (25%).



(a)



(b)

Fig. 3. Intercomparison of aerosol backscatter profiles at 532 nm between Munich (mu) and Thessaloniki (th) taken on (a) 22 September 2000 at 18:10–18:15 UT and (b) 23 September 2000 at 9:40–9:45 UT.

nm, whereas the IFT and MIM systems used three-wavelength Nd:YAG lasers.

In Tables 4–6 the mean deviations and standard deviations are given, together with the values for wavelengths and height ranges, from 11 August 1998 at 12:07–12:12 UT and from 9 August 1998 at 22:30–23:00 UT. In the latter case the allowed relative deviations were exceeded in the PBL, but on that day

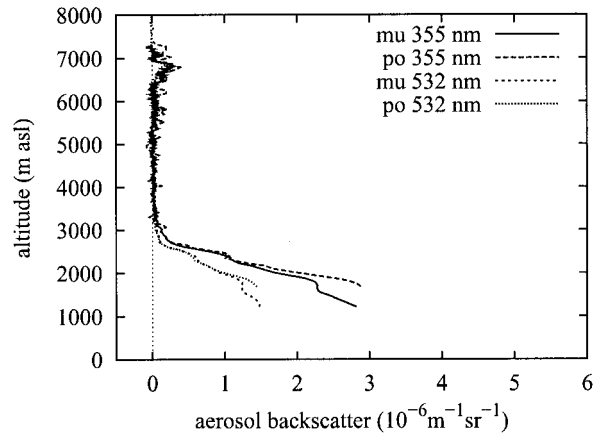


Fig. 4. Intercomparison of aerosol backscatter profiles at 355 and 532 nm between Munich (mu) and Potenza (po) taken on 10 October 2000 at 16:20–17:02 UT.

the aerosol load was low, and all deviations stayed within the allowed absolute limits.

b. Munich–Thessaloniki Data

The Munich–Thessaloniki intercomparisons had to be restricted to 532 nm, because instabilities in the system from Thessaloniki made reliable measurements at 355 nm impossible. Thermal drifts of the alignment were also detected at 532 nm. These drifts led to changing overlap functions, and three of the four intercomparisons were made at altitudes above 2000 m asl. However, on September 22 the lowest compared altitude was 1200 m.

Figure 3 shows comparisons of two sets of measurements, from 22 September at 18:10–18:15 and from 23 September 23 at 9:40–9:45. Generally, the deviations are small and stay well below the given limits. Differences of ~ 30 m in the observed height of the aerosol layer can be seen in parts of the profiles. The probing of different air parcels by the two systems during rapidly changing conditions of aerosol backscatter explains the differences. Only short episodes of cloud-free profiles were possible on those two days. The deviations for four cases are given in Table 7.

Table 7. Munich and Thessaloniki Backscatter Intercomparisons^a

Date (UT)	Height Range (m)	Mean Deviation ($10^{-6} \text{ m}^{-1} \text{ sr}^{-1}$)	Standard Deviation ($10^{-6} \text{ m}^{-1} \text{ sr}^{-1}$)
22/09/2000 (18:10–18:15)	1200–4000	0.05/2.2%	0.21/9.5%
	4300–7000	0.02	0.04
23/09/2000 (9:40–9:45)	2000–3200	0.01/0.3%	0.36/19.2%
	3400–6500	0.02	0.04
23/09/2000 (10:05–10:25)	2000–3300	0.18/10.6%	0.24/13.8%
	3400–7000	0.00	0.03
23/09/2000 (11:20–11:50)	2000–3000	0.14/8.9%	0.16/10.5%
	3300–7000	0.03	0.04

^aAllowed absolute mean deviations and standard deviations are $0.5 \times 10^{-6} \text{ m}^{-1} \text{ sr}^{-1}$. Allowed relative mean (and standard) deviations in the PBL are 20% (25%). Wavelength, 532 nm.

Table 8. Munich and Potenza Backscatter Intercomparisons^a

Date (UT)	Wavelength (nm)	Height Range (m)	Mean Deviation ($\times 10^{-6} \text{ m}^{-1} \text{ sr}^{-1}$)	Standard Deviation ($\times 10^{-6} \text{ m}^{-1} \text{ sr}^{-1}$)
10/10/2000 (16:20–17:02)	355	1800–2500	-0.21/-14.1%	0.28/19.0%
		3000–7000	-0.02	0.07
10/10/2000 (16:20–17:02)	532	1800–2500	-0.03/3.2%	-0.07/8.3%
		3000–7000	0.01	0.03
11/10/2000 (10:21–10:28)	355	1800–3500	-0.06/3.8%	0.20/12.7%
		4000–5500	0.03	0.22
11/10/2000 (10:21–10:28)	532	1800–3500	-0.02/-2.7%	0.07/8.1%
		4000–9000	-0.01	0.08
11/10/2000 (11:58–12:02)	355	1700–3500	-0.03/-1.8%	0.14/8.0%
		4000–5000	0.03	0.30
11/10/2000 (11:58–12:02)	532	1700–3500	-0.04/-4.1%	0.11/12.5%
		4000–7500	-0.01	0.14

^aAllowed absolute mean deviations and standard deviations are $0.5 \times 10^{-6} \text{ m}^{-1} \text{ sr}^{-1}$ at both wavelengths. Allowed relative mean (and standard) deviations in the PBL are 20% (25%) at both wavelengths.

c. Munich–Potenza Data

The intercomparisons of Munich and Potenza taken in October 2000 also suffered from bad weather conditions; therefore only on 10 October could a longer average of 40 min be taken (Fig. 4). The following day, only shorter periods in cloud gaps were used for the intercomparisons. Potenza is 820 m asl; the lowest point with full overlap was ~ 1000 m above ground level, so the measurements at altitudes above ~ 1800 m asl were compared.

At both wavelengths, only minor deviations between the systems were detected (Table 8). The lowest measurement heights were affected mostly by some smaller differences, which could have been due to overlap effects or to detector nonlinearities. However, the differences remained small and did not affect the good performance that both systems showed during this intercomparison.

d. Hamburg–Neuchâtel Data

The three-wavelength aerosol Raman lidar of MPI was compared with the microlidar of the Observatoire Cantonal Neuchâtel in September 2000 at Palaiseau. The microlidar emitted at a very high repetition rate (11 kHz) and a very low pulse energy ($\approx 1 \mu\text{J}$) at 532 nm. Because of this low pulse energy the microlidar is limited in range in the daytime. Two of the intercomparison episodes were taken at night when profiles could be measured at heights of more than 9000 m. During the daytime the microlidar data can be used with good accuracy up to 4000–5000 m. With the low output energy of the laser used for the microlidar in mind, this is a fairly good result. All absolute deviations were within the allowed limits; only on 11 September did the relative error of the aerosol backscatter exceed the limits because of the prevailing low backscatter. Figure 5 shows the daytime profile from 13 September 2000 and a nighttime profile from 11 September 2000. In Table 9 the mean and standard deviations can be found, together with data on a third case from 14 September 2000.

2. Aerosol Extinction

a. Hamburg–Leipzig Data

Extinction profiles for Hamburg and Leipzig derived from the Raman method were compared. One pro-

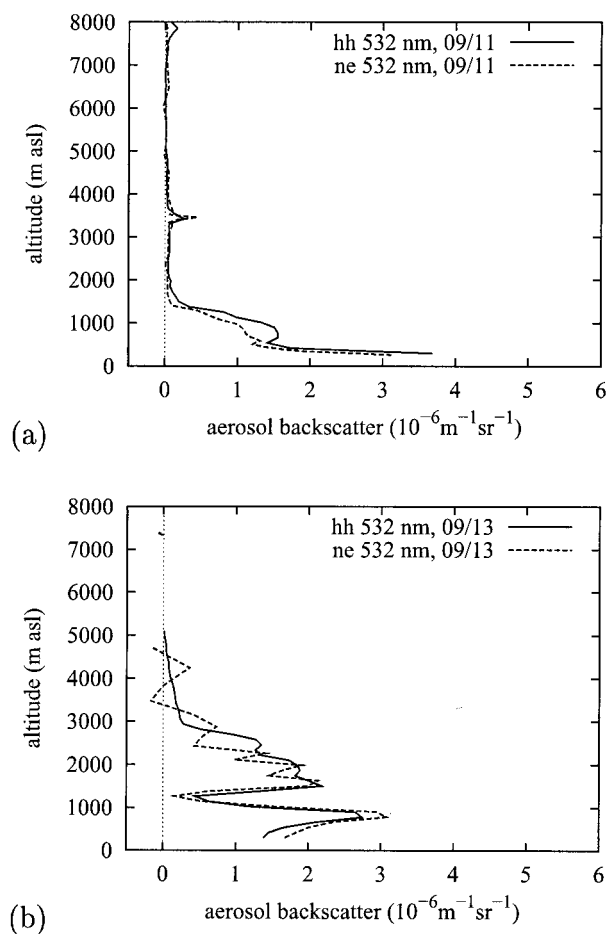


Fig. 5. Intercomparison of aerosol backscatter profiles at 532 nm between Hamburg (hh) and Neuchâtel (ne) taken on (a) 11 September 2000 at 19:40–20:00 UT and (b) 13 September at 14:51–15:08 UT.

Table 9. Hamburg and Neuchâtel Backscatter Intercomparisons^a

Date (UT)	Height Range (m)	Mean Deviation ($\times 10^{-6} \text{ m}^{-1} \text{ sr}^{-1}$)	Standard Deviation ($\times 10^{-6} \text{ m}^{-1} \text{ sr}^{-1}$)
11/09/2000 (19:40–20:00)	400–1300	0.34/33.3%	0.37/36.9%
	2000–9800	0.02	0.05
13/09/2000 (14:51–15:08)	300–2400	0.02/1.5%	0.36/21.9%
	2500–4700	0.03	0.29
14/09/2000 (20:30–21:00)	300–1300	-0.37/-17.9%	0.40/19.3%
	1500–9000	0.03	0.05

^aAllowed absolute mean deviations and standard deviations are $0.5 \times 10^{-6} \text{ m}^{-1} \text{ sr}^{-1}$. Allowed relative mean (and standard) deviations in the PBL are 20% (25%). Wavelength, 532.

file had already been taken in 1998 during the LACE 98 experiment. It is shown in Fig. 6 and was taken in the same time interval as some of the backscatter measurements described in Section 1. The agreement can be regarded as excellent: The mean deviation is only 4.7%, with a standard deviation of 11.7% (Table 10).

b. Hamburg–Aberystwyth Data

The two systems from Hamburg and Aberystwyth operate the nitrogen Raman channel at 387 nm, so aerosol extinction profiles could be determined and compared. Measurements were taken mostly to nighttime because the Raman channels can be operated only with very low background light. Both systems had to deal with problems with data from their large far-range telescope at 355 nm: the MPI sys-

tem with electronic interference, and the University of Aberystwyth with the adjustment of the telescope. The latter could be corrected after the experiment, which improved the data quality of this EARLINET station.

The electronics problem in the MPI system could also be solved after the experiment. So most of the profiles shown here were measured with a small near-range telescope and were limited in range. High standard deviations in the upper heights are due to the low signal level achieved with the small telescope. Good agreement could be found for the average values of the extinction profiles in the PBL; the mean deviations were 2.1% and 0.2%, respectively, on 6 May and 7 May 2001, for Hamburg and Aberystwyth, The standard deviation shows high relative deviations of as much as 35%, but they stayed within the predefined maximum absolute deviation of $1.0 \times 10^{-4} \text{ m}^{-1}$ (Fig. 7 and Table 11).

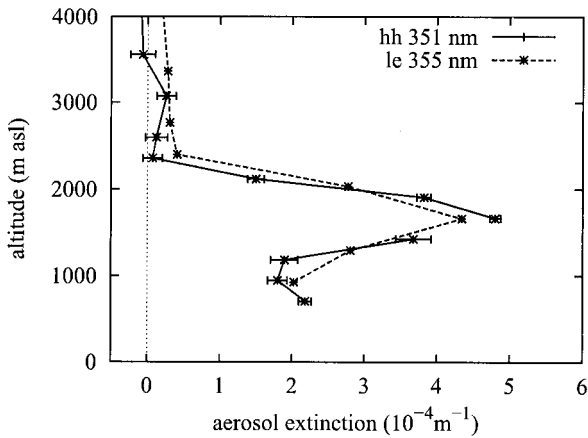


Fig. 6. Intercomparison of aerosol extinction profiles at 355 nm between Hamburg (hh) and Leipzig (le) taken on 11 August 1998 at 21:15–21:45 UT.

B. Intercomparison of Lidar and Photometer

During nighttime, Raman lidar can deliver aerosol extinction profiles with high accuracy. If the measurements cover a significant part of the planetary boundary layer, the aerosol optical depth (AOD) can be derived by integration of the extinction over the whole height range from ground to the top of the profile. Assuming that the planetary boundary layer is still well mixed at 1 or 2 h after sunset, the extinction profile can be extrapolated to ground without large errors if constant extinction values are used.

These measurements can best be compared with starphotometer measurements that can be performed simultaneously, but this instrument is not frequently operated on a routine basis. In contrast, automatically operating sunphotometers are quite of-

Table 10. Hamburg and Leipzig Extinction Intercomparisons on 11/08/1998^a

UT on 11/08/1998	Wavelength (nm)		Height Range (m)	Mean Deviation ($\times 10^{-4} \text{ m}^{-1}$)	Standard Deviation ($\times 10^{-4} \text{ m}^{-1}$)
	Leipzig	Hamburg			
(21:15–21:45)	355	351	600–2000	0.05/4.7%	0.34/11.7%
			2400–3800	0.17	0.25

^aAllowed absolute mean (and standard) deviations are $0.5 (1.0) \times 10^{-4} \text{ m}^{-1}$. Allowed relative mean (and standard) deviations in the PBL are 20% (25%).

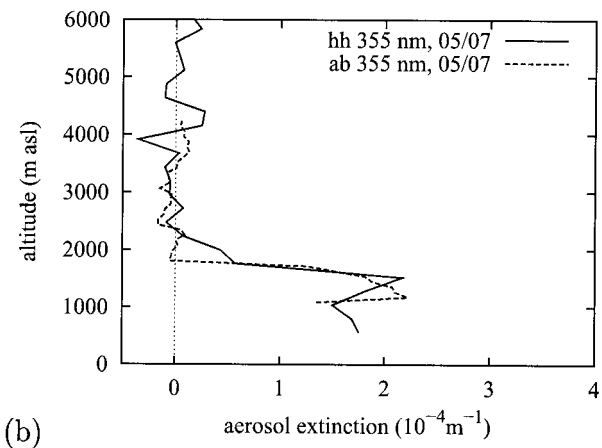
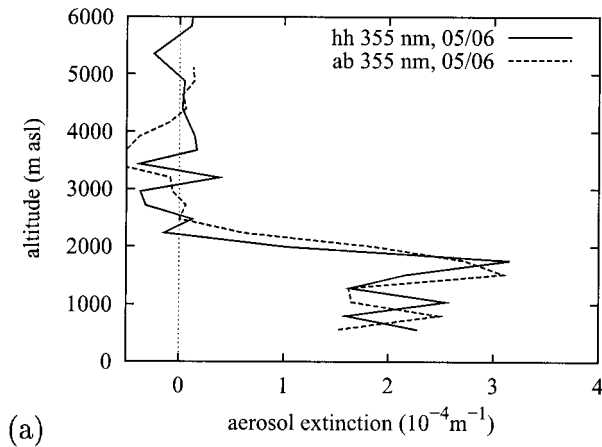


Fig. 7. Intercomparison of aerosol extinction profiles at 355 nm between Hamburg (hh) and Aberystwyth (ab) taken on (a) 6 May 2001 at 20:30–20:45 UT and (b) 7 May 2001 at 20:44–21:44 UT.

ten available,³⁴ and lidar systems can be compared with those instruments. The comparisons have to be treated carefully, because a time delay of approximately 2–3 h between the last measurement of the sunphotometer in daytime and the first Raman lidar measurement at nighttime cannot be avoided. Additionally, cirrus clouds can prevent accurate sunphotometer measurements. However, from continuous lidar measurements, the development of the aerosol distribution and the presence of cirrus clouds can be observed, which permit intercomparisons without large systematic errors in some situations.

The aerosol optical depth from the MPI Raman

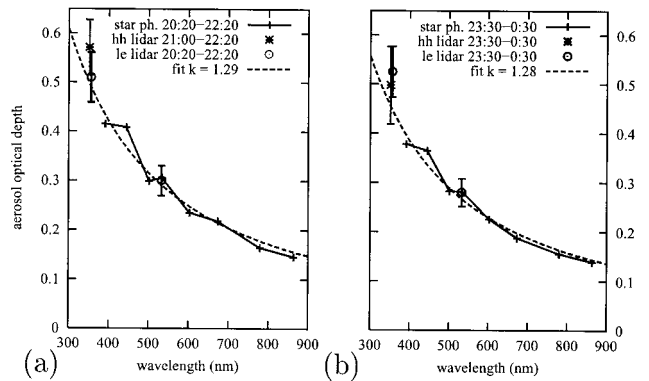


Fig. 8. Intercomparison of aerosol optical depth measurements with the MPI Raman lidar (hh), the IFT Raman lidar (le), and the starphotometer from Meteorologisches Observatorium Lindenberg on 11–12 August 1998. Photometer error bars are of the order of 0.01–0.02 for all wavelengths.

lidar and the IFT transportable Raman lidar were compared to photometer data. Figure 8 shows the intercomparison of the lidar optical depth with starphotometer measurements performed in Lindenberg during LACE 98 for two episodes during the night of 11–12 August 1998. The 532-nm optical depth from IFT fits the starphotometer almost perfectly; also, the extrapolation of the photometer data to shorter wavelengths near 355 nm assuming a spectrally constant Ångström exponent gives agreement between the two instruments within the error bars of the lidar measurements of 0.05–0.08. The lidar profiles were extrapolated down to ground, assuming a height-constant aerosol extinction in the lowest 500 m. The error that resulted from this assumption is estimated to be 0.025 in the optical depth, corresponding to 25% of the optical depth of this layer.

During the intercomparison experiment in Palaiseau, the MPI Raman lidar could also be compared to the automatic sunphotometer from the Laboratoire Météorologie Dynamique, Palaiseau, on two days. In Figure 9 the optical depth measurements from the sunphotometer are plotted at four measured wavelengths from 440 to 1020 nm. Assuming again that the AOD follows an Ångström law ($AOD \propto \lambda^{-k}$), the measurements were extrapolated to lower wavelengths, although this was done because of additional errors that are due to insufficient knowledge about the wavelength dependence of the aerosol optical depth at wavelengths below 400 nm. The given er-

Table 11. Hamburg and Aberystwyth Extinction Intercomparisons^a

Date (UT)	Height Range (m)	Mean Deviation ($\times 10^{-4} \text{ m}^{-1}$)	Standard Deviation ($\times 10^{-4} \text{ m}^{-1}$)
06/05/2001 (20:30–20:45)	500–1800	0.05/2.1%	0.79/35.5%
	2400–5000	0.13	0.36
07/05/2001 (20:44–21:44)	1100–1800	–0.04/–0.2%	0.32/20.8%
	2400–4000	–0.06	0.21

^aAllowed absolute mean (and standard) deviations are $0.5 (1.0) \times 10^{-4} \text{ m}^{-1}$. Allowed relative mean (and standard) deviations in the PBL are 20% (25%). Wavelength, 355 nm.

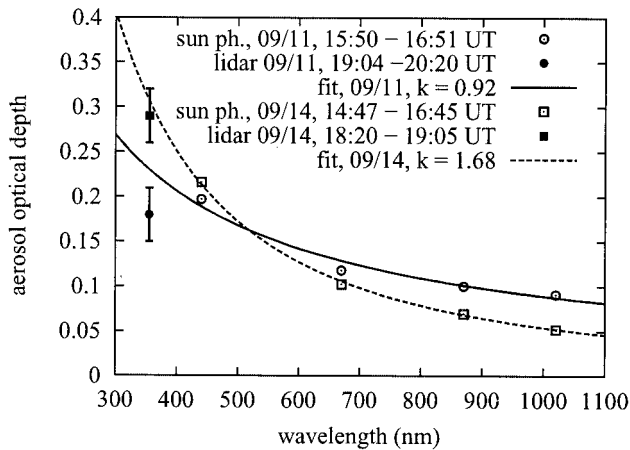


Fig. 9. Intercomparison of aerosol optical depth measurements with the MPI Raman lidar and the sunphotometer from the Laboratoire Météorologie Dynamique, Palaiseau. Photometer error bars are estimated to 0.02, excluding extrapolation errors.

ror of the lidar data contains the statistical measurement error and the error in the optical depth of the lowest part of the atmosphere, where the lidar cannot deliver extinction values. A typical overall error in the lidar data is ~ 0.05 . The accuracy of the sunphotometer's optical depth data is usually of the order of 0.01–0.02.³⁴

Keeping in mind the potential error sources mentioned above, the measurements of 11 and 14 September 2000 show agreement within the error bars. For the sunphotometer, late-afternoon periods with fairly constant optical depth were averaged. The lidar data were taken after sunset, and 45–70-min averages were used in deriving the aerosol extinction profile, which led to small statistical errors of the extinction. The largest error came from the unknown extinction values in the lowest part of the boundary layer. The presence of cirrus in the photometer data, which would lead to too-high optical depth values, can never be completely excluded. However, the lidar data did not show cirrus clouds throughout the measurement period of the sunphotometer on both days.

6. Overview of the Results

The whole set of intercomparison experiments turned out to be a good and hard test for all systems. In several cases the systems could be improved after the measurements. Many of the existing problems certainly would not have been detected without the intercomparison measurements. Besides, a high quality of the measurements could be stated in almost all cases and the predefined goals could be reached. Figures 10 and 11 give the absolute and relative mean deviations and standard deviations in the PBL for all aerosol backscatter intercomparisons used for the EARLINET quality assurance. Almost all relative values are well within the 20% limits, most of them even within $\pm 10\%$. Only two cases have significantly higher deviations in the PBL.

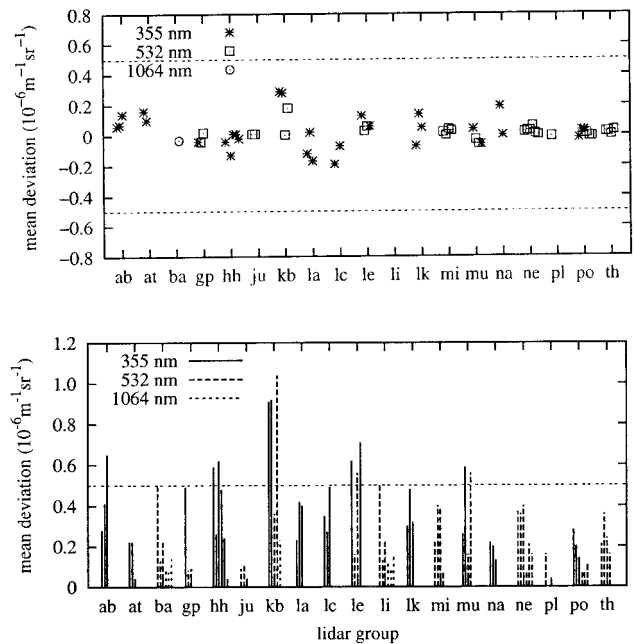


Fig. 10. Absolute values of the mean deviations and standard deviations of all aerosol backscatter intercomparisons in the PBL.

However, those cases are connected with low aerosol load, and the absolute deviations stay well below the allowed value of $0.5 \times 10^{-6} \text{ m}^{-1} \text{ sr}^{-1}$.

In some cases the standard deviations exceed the 25% margin. Again, these cases generally are connected with low aerosol loads, and the absolute deviations still are acceptable. Sometimes an overestimation of the errors occurs if small differences in height are being detected. The point-to-point calculation of the differences that was used can

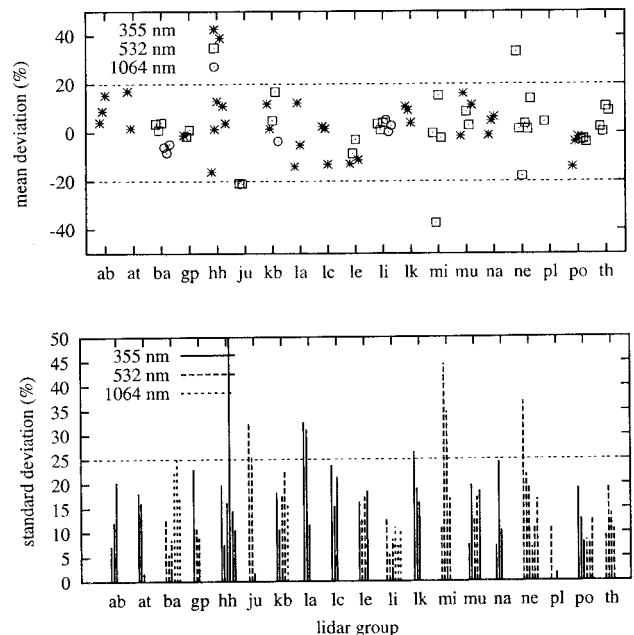


Fig. 11. Relative values of the mean deviations and standard deviations of all aerosol backscatter intercomparisons in the PBL.

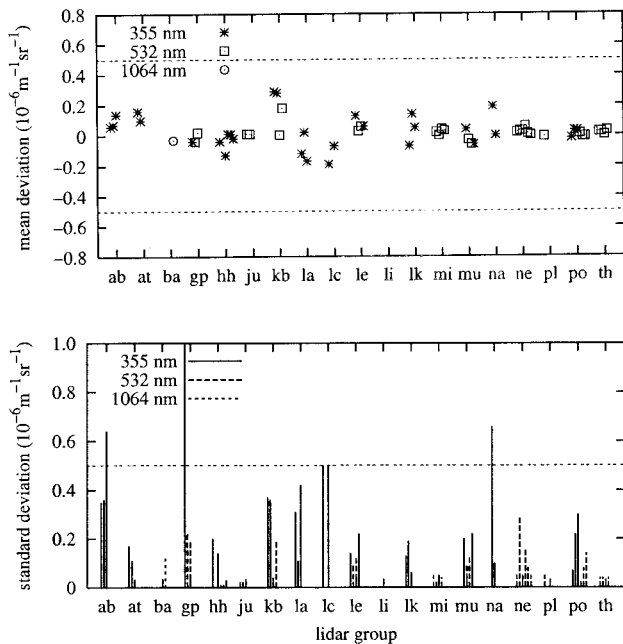


Fig. 12. Absolute values of the mean deviations and standard deviations of all aerosol backscatter intercomparisons in the FT.

lead to quite large differences if strong gradients occur in the aerosol profile.

The absolute deviations of all compared profiles in regions with low aerosol are displayed in Fig. 12. Here, in almost all cases mean deviations stay below $0.2 \times 10^{-6} \text{ m}^{-1} \text{ sr}^{-1}$, and this value holds for the standard deviation, too. Where higher standard deviations have been detected, higher averaging, especially in height, would lead to smaller fluctuations. Because often little variability is seen in the upper tropospheric aerosol profiles, larger vertical averaging would be an appropriate procedure with which to increase the data quality in higher altitudes.

Aerosol extinction profiles could be compared in only two cases. For the EARLINET, the MPI lidar was the only transportable Raman lidar system that could be used for intercomparison. However, the effort to move the MPI system was much higher than for the system from Munich; therefore the MIM system, although it was not equipped with Raman channels, was chosen to travel to Italy and Greece. In Italy, all systems perform Raman measurements but none of them is transportable. The extinction profiles from MPI and IFT taken in 1998 showed a mean deviation of only 5% and 12% standard deviation. The extinction profiles measured by MPI and the University of Aberystwyth in May 2001 showed a larger standard deviation of as much as 35% in one case, but the allowed absolute limits were not exceeded. Good agreement was found for the mean values of the profiles that stayed much below 5% in the PBL. Additionally, the MPI Raman lidar and the IFT transportable Raman lidar were compared to starphotometer measurements in Lindenberg; the MPI system was compared to sunphotometer measurements in Palaiseau as well. Despite the diffi-

culties connected with these comparisons, the agreement was good and stayed within the error bars of 0.05–0.08. This result demonstrates the high quality of the lidar data which also holds when widely different instruments are used.

7. Summary

To achieve the goals of EARLINET it is essential to provide aerosol backscatter and extinction profiles on a quantitative basis. To derive those quantities, 19 European lidar groups operate aerosol lidar systems that are quite different in detail. To achieve a homogeneous data set, and to make sure that all systems and the algorithms used for the evaluation work well, a large number of intercomparison experiments were performed that tested at least two systems at a time at one place. Algorithms were tested separately by use of synthetic lidar data as input and recalculation of the assumed aerosol distribution. The results have been discussed in detail by Böckmann *et al.*¹⁸

The instrument intercomparison included all lidar testing groups with 19 lidar systems. Eighteen of these lidar groups compared their systems with quality-assured lidar systems. One (the Minsk system) made internal intercomparisons of two of its lidar systems operating at the same place and the same wavelength. In 16 cases the predefined quality criteria could be met from the beginning. The aerosol backscatter measurements showed deviations of less than 10% in most cases. The standard deviations were typically below 25%. Higher deviations were always connected with low aerosol loads and did not exceed the maximum allowed absolute deviation in those cases. System precision, including algorithms, could be estimated to be better than 20% in many cases and to even better than 10% in the PBL. Above that layer, absolute deviations were typically of the order of $0.1 \times 10^{-6} \text{ m}^{-1} \text{ sr}^{-1}$ or better, which are less than 10% of low aerosol values in the PBL. Keeping in mind that errors in the determination of the aerosol backscatter profile by use of pure elastic backscatter at 355 nm can be as large as 50% if no information about the lidar ratio can be provided from Raman measurements, these errors are quite small. Calculation errors that were due to the use of different averaging procedures and algorithm implementations also contributed to the total error. They were of the order of 2–4%; see Part 2 of this series.¹⁸

Intercomparisons of Raman extinction measurements could be made only in two cases. Aerosol extinction profiles in the UV derived from those systems during the LACE 98 campaign showed excellent agreement, with mean deviations of 5% and a standard deviation of 12% for 0.5-h measurement. The comparisons of the MPI and the University of Aberystwyth data showed good agreement of the extinction profiles, but the standard deviation of the measured extinction was rather large. However, large standard deviations are not unusual for Raman measurements because of the weak backscattered signal. Mean deviations were below 5% in both cases ana-

lyzed, a result that permits accurate determination of the aerosol optical depth, as well.

The AOD from aerosol extinction profiles of the MPI lidar was compared to sunphotometer measurements during the intercomparison campaign in Palaiseau. The IFT and MPI lidars were also compared to starphotometer measurements during LACE 98. In all cases the agreement was good (within 0.05 aerosol optical depth), especially if one considers the difficulties of such intercomparisons, beginning with the different optical path, the unknown wavelength dependence in the UV, and the time difference of 2–3 h in the sunphotometer measurements. This result shows that optical depth measurements can be made with lidar systems. From lidars, even vertically resolved profiles can be derived, and measurements can be taken also in presence of high-level clouds.

Although good intercomparison results could be achieved, some of the systems tested had to be improved. The detected errors were due mainly to detector saturation, overlap problems, or thermal instabilities. The problems were solved in most cases; however, sometimes the lidar groups had to determine the validity ranges of their data carefully and apply further improvements (e.g., to thermal stabilization) to their systems. In this sense the intercomparisons showed that good agreement can be achieved but also that great care has to be taken to maintain this quality during the routine operation of the lidar systems.

In three cases the system intercomparisons failed in the first attempt. Major system reconstructions were recommended in these cases, which were completed in 2001 (Linköping) and 2002 (Lisbon and Palaiseau). New intercomparison experiments showed that the new systems perform much better and deliver reliable results for the EARLINET data base.

The financial support of this research by the European Commission under grant EVR1-CT-1999-40003 is gratefully acknowledged. We thank the Swiss Federal Office for Education and Sciences for support of the Observatoire Cantonal Neuchâtel (contract 99.0650-1) and of the Ecole Polytechnique Fédérale de Lausanne (contract 582.607).

We thank the scientific and technical staff of the Meteorological Observatory Lindenberg for very good support during the LACE 98 campaign when the intercomparisons of the German aerosol lidar systems were made. Starphotometer data was provided by Ulrich Leiterer and Victor Novikov. That campaign was funded by the German Federal Minister for Education and Research within the "Atmospheric Aerosol Research" program.

We are grateful to the Federated Instrument Network and Data Archive for Aerosol Characterization and to Bernadette Chatenet for providing sunphotometer data for the intercomparison of the optical depth.

References

1. J. Bösenberg, A. Ansmann, J. M. Baldasano, D. Balis, C. Böckmann, B. Calpini, A. Chaikovskiy, P. Flamant, A. Hagard, V. Mitev, A. Papayannis, J. Pelon, D. Resendes, J. Schneider, N. Spinelli, T. Trickl, G. Vaughan, G. Visconti, and M. Wiegner, "EARLINET: a European aerosol research lidar network," in *Laser Remote Sensing of the Atmosphere*, A. Dabas, C. Loth, and J. Pelon, eds., selected papers of the 20th International Laser Radar Conference (Edition Ecole Polytechnique, Palaiseau, France, 2001), pp. 155–158.
2. G. C. Grabbe, J. Bösenberg, H. Dier, U. Görndorf, V. Matthias, G. Peters, T. Schaberl, and C. Senff, "Intercomparison of ozone measurements between lidar and ECC-sondes," *Contr. Atmos. Phys.* **69**, 189–203 (1996).
3. A. Apituley, "Comparison of the RIVM tropospheric ozone lidar to *in situ* measuring instruments using data acquired during TROLIX," Rep. 722701001 (Rijksinstituut voor Volksgezondheid en Milieu, Bilthoven, The Netherlands, 1995).
4. J. Bösenberg, G. Ancellet, A. Apituley, H. Bergwerff, G. von Cossart, H. Edner, J. Fiedler, B. Galle, C. N. de Jonge, J. Melquist, V. Mitev, T. Schaberl, G. Sonnemann, J. Spaakman, D. J. P. Swart, and E. Wallinder, "Tropospheric Ozone Lidar Intercomparison Experiment, TROLIX'91, field phase report." Rep. 102 (Max-Planck-Institut für Meteorologie, Hamburg, Germany, 1993).
5. I. S. McDermid, S. M. Godin, and D. T. Walsh, "Lidar measurements of stratospheric ozone and intercomparisons and validation," *Appl. Opt.* **29**, 4914–4923 (1990).
6. I. S. McDermid, S. M. Godin, R. A. Barnes, C. L. Parsons, A. Torres, M. P. McCormick, W. P. Chu, P. Wang, J. Butler, P. Newman, J. Burris, R. Ferrare, D. Whitemann, and T. J. McGee, "Comparison of ozone profiles from ground-based lidar, electrochemical concentration cell balloon sonde, ROCOZ, a rocket ozonesonde, and stratospheric aerosol and gas experiment satellite measurements," *J. Geophys. Res.* **95**, 10037–10042 (1990).
7. R. A. Ferrare, D. N. Whiteman, S. H. Melfi, K. D. Evans, F. J. Schmidlin, and D. O'C. Starr, "A comparison of water vapor measurements made by Raman lidar and radiosondes," *J. Atmos. Ocean. Technol.* **12**, 1177–1195 (1995).
8. V. Sherlock, A. Garnier, A. Hauchecorne, and P. Keckhut, "Implementation and validation of a Raman lidar measurement of middle and upper tropospheric water vapor," *Appl. Opt.* **38**, 5838–5850 (1999).
9. H. Steinhagen, S. Bakan, J. Bösenberg, H. Dier, D. Engelbart, J. Fischer, G. Gendt, U. Görndorf, J. Güldner, F. Jansen, V. Lehmann, U. Leiterer, J. Neisser, and V. Wulfmeyer, "Field campaign LINEX 96/1—possibilities of water vapor observation in the free atmosphere," *Meteorol. Z.* **6**, 377–391 (1998).
10. I. S. McDermid, S. M. Godin, L. O. Lindqvist, T. D. Walsh, J. Burris, J. Butler, R. Ferrare, D. Whitemann, and T. J. McGee, "Measurement intercomparison of the JPL and GSFC stratospheric ozone lidar systems," *Appl. Opt.* **29**, 4671–4676 (1990).
11. H. Linné, D. D. Turner, J. E. M. Goldsmith, T. P. Tooman, J. Bösenberg, K. Ertel, and S. Lehmann, "Intercomparison of DIAL and Raman lidar measurements of humidity profiles," in A. Dabas, C. Loth, and J. Pelon, eds., *Laser Remote Sensing of the Atmosphere*, selected papers of the 20th International Laser Radar Conference (Edition Ecole Polytechnique, Palaiseau, France, 2001), pp. 293–298.
12. S. Gassó and D. A. Hegg, "Comparison of columnar aerosol optical properties measured by the MODIS airborne simulator with *in situ* measurements: a case study," *Remote Sens. Environ.* **66**, 592–593 (1998).
13. U. Wandinger, D. Müller, C. Böckmann, D. Althausen, V. Matthias, J. Bösenberg, V. Weiss, M. Fiebig, M. Wendisch, A. Stohl, and A. Ansmann, "Optical and microphysical characterization of biomass-burning and industrial-pollution aerosols from multiwavelength lidar and aircraft measurements," *J. Geophys. Res.* **107**, 10.1029/2000JD000202 (2002).

14. R. Ferrare, S. H. Melfi, D. N. Whiteman, K. D. Evans, and R. Leifer, "Raman lidar measurements of aerosol extinction and backscattering. 2. Derivation of aerosol real refractive index, single-scattering albedo, and humidification factor using Raman lidar and aircraft size distribution measurements," *J. Geophys. Res.* **103**, 19673–19689 (1998).
15. R. Ferrare, S. H. Melfi, D. N. Whiteman, K. D. Evans, and R. Leifer, "Raman lidar measurements of aerosol extinction and backscattering. 1. Methods and comparisons," *J. Geophys. Res.* **103**, 19663–19672 (1998).
16. A. Ansmann, F. Wagner, D. Althausen, D. Müller, A. Herber, and U. Wandinger, "European pollution outbreaks during ACE 2: lofted aerosol plumes observed with Raman lidar at the Portuguese coast," *J. Geophys. Res.* **106**, 20725–20733 (2001).
17. A. Ansmann, U. Wandinger, A. Wiedensohler, and U. Leiterer, "Lindenberg aerosol characterization experiment 1998 (LACE 98): overview," *J. Geophys. Res. D* **107**, 10.1029/2000JD000233 (2002).
18. C. Böckmann, U. Wandinger, A. Ansmann, J. Bösenberg, V. Amiridis, A. Boselli, A. Delaval, F. De Tomasi, M. Frioud, A. Hågård, M. Iarlori, L. Komguem, S. Kreipl, G. Larchevêque, V. Matthias, A. Papayannis, G. Pappalardo, F. Rocadenbosch, J. Schneider, V. Shcherbakov, and M. Wiegner, "Aerosol lidar intercomparison in the frame of the EARLINET project. 2. Aerosol backscatter algorithms," *Appl. Opt.* **43**, 977–989 (2004).
19. G. Pappalardo, A. Amodeo, M. Pandolfi, U. Wandinger, A. Ansmann, J. Bösenberg, V. Matthias, F. DeTomasi, M. Frioud, M. Iarlori, L. Komguem, A. Papayannis, F. Rocadenbosch, and X. Wang, "Aerosol lidar intercomparisons in the framework of EARLINET. 3. Raman lidar algorithm for aerosol extinction, backscatter, and lidar ratio," *Appl. Opt.*, submitted for publication.
20. J. D. Klett, "Stable analytical inversion solution for processing lidar returns," *Appl. Opt.* **20**, 211–220 (1981).
21. J. D. Klett, "Lidar inversion with variable backscatter/extinction ratios," *Appl. Opt.* **24**, 1638–1643 (1985).
22. F. G. Fernald, B. M. Herman, and J. A. Reagan, "Determination of aerosol height distributions by lidar," *J. Appl. Meteorol.* **11**, 482–489 (1972).
23. F. G. Fernald, "Analysis of atmospheric lidar observations: some comments," *Appl. Opt.* **23**, 652–653 (1984).
24. B. Edlen, "The dispersion of standard air," *J. Opt. Soc. Am.* **43**, 339 (1953).
25. L. Elterman, "UV, visible, and IR attenuation for altitudes to 50 km, 1968," Environmental Research Paper 285, AFCRL-68-0153 (U.S. Air Force Research Laboratory, Cambridge, Mass., 1968).
26. B. A. Bodhaine, N. B. Wood, E. G. Dutton, and J. R. Slusser, "On Rayleigh optical depth calculations," *J. Atmos. Ocean. Technol.* **16**, 1854–1861 (1999).
27. Y. Sasano, E. V. Browell, and S. Ismail, "Error caused by using a constant extinction/backscattering ratio in the lidar solution," *Appl. Opt.* **24**, 3929–3932 (1985).
28. V. A. Kovalev and H. Moosmüller, "Distortion of particulate extinction profiles measured with lidar in a two-component atmosphere," *Appl. Opt.* **33**, 6499–6507 (1994).
29. M. Matsumoto and N. Takeuchi, "Effects of misestimated far-end boundary values on two common lidar inversion solutions," *Appl. Opt.* **33**, 6451–6456 (1994).
30. J. Bösenberg, R. Timm, and V. Wulfmeyer, "Study on retrieval algorithms for a backscatter lidar," Final Rep. 226 (Max-Planck-Institut für Meteorologie, Hamburg, Germany, 1997).
31. A. Ansmann, U. Wandinger, M. Riebesell, C. Weitkamp, and W. Michaelis, "Independent measurement of extinction and backscatter profiles in cirrus clouds by using a combined Raman elastic-backscatter lidar," *Appl. Opt.* **31**, 7113–7131 (1992).
32. J. Bösenberg, M. Alpers, D. Althausen, A. Ansmann, C. Böckmann, R. Eixmann, A. Franke, V. Freudenthaler, H. Giehl, H. Jäger, S. Kreipl, H. Linné, V. Matthias, I. Mattis, D. Müller, J. Sarközi, L. Schneidenbach, J. Schneider, T. Trickl, E. Vorobieva, U. Wandinger, and M. Wiegner, "The German aerosol lidar network: methodology, data, analysis," Rep. 317 (Max-Planck-Institut für Meteorologie, Hamburg, Germany, 2001).
33. D. Althausen, D. Müller, A. Ansmann, U. Wandinger, H. Hube, E. Clauer, and S. Zörner, "Scanning six-wavelength eleven-channel aerosol lidar," *J. Atmos. Ocean. Technol.* **17**, 1469–1482 (2000).
34. B. N. Holben, T. F. Eck, I. Slutsker, D. Tanré, J. P. Buis, A. Setzer, E. Vermote, J. A. Reagan, Y. J. Kaufman, T. Nakajima, F. Lavenu, I. Jankowiak, and A. Smirnov, "AERONET—a federated instrument network and data archive for aerosol characterization," *Remote Sens. Environ.* **66**, 1–16 (1998).